Boosting the Efficiency

IMAGE LICENSED BY INGRAM PUBLISHING

Alírio Boaventura, Daniel Belo, Ricardo Fernandes, Ana Collado, Apostolos Georgiadis, and Nuno Borges Carvalho

Traditionally, wireless power is delivered through single-carrier, continuous-wave (CW) signals. Most research efforts to enhance the efficiency of wireless power transfer systems have been confined to the circuit-level design. However, in recent years, attention has been paid to the waveform design for wireless power transmission. It has been found that signals featuring a high peak-to-average power ratio (PAPR) can provide efficiency improvement when compared with CW signals. A number of approaches have been proposed, such as multisines/multicarrier orthogonal frequency division multiplex (OFDM) signals, chaotic signals, harmonic signals, ultrawideband (UWB) signals, intermittent CW (ICW) signals, or white-noise signals. This article reviews these techniques with a focus on multisines/multicarrier signals, harmonic signals, and chaotic signals. A theoretical explanation for efficiency improvement is provided and accompanied by experimental results. Circuit design considerations are presented for the receiver side, and efficient transmission architectures are also described with an emphasis on spatial power combining.

Wireless Power Waveforms

Power transfer without wires has been carried out for many years using single-carrier CW signals. However, it has been demonstrated recently that proper waveform design (e.g., featuring high PAPR) can improve the efficiency of wireless energy transfer, especially for low power levels. Curiously, the first electromagnetic wave that was successfully generated, transmitted, and detected by Heinrich Hertz in 1887 was in fact a nonconstant envelope signal, consisting of damped waves [1]. This type of signal was used for many years for signal transmission (in wireless telegraphy) and also in some wireless power transfer experiments

Alírio Boaventura (a34422@ua.pt), Daniel Belo, Ricardo Fernandes, and Nuno Borges Carvalho are with the Instituto de Telecomunicações, Departmento de Electrónica, Telecomunicações e Informatica, Universidade de Aveiro, Aveiro, Portugal. Ana Collado (acollado@cttc.es) and Apostolos Georgiadis (ageorgiadis@cttc.es) are with the Centre Tecnologic de Telecomunicacions de Catalunya (CTTC), Castelldefels, Spain.

Digital Object Identifier 10.1109/MMM.2014.2388332
Date of publication: 6 March 2015

Signals featuring a high peak-to-average power ratio can provide efficiency improvement when compared with CW signals.

performed by Nikola Tesla in 1894 and the following years [2]. Nevertheless, damped waves, which present a large spectrum occupancy, were later replaced by CW signals, first generated in 1902 by Ernst Alexanderson's high-frequency alternators [3]. The CW signals have been the choice for wireless power transmission (WPT) applications since WPT experiments were resumed by W. Brown in the 1960s (some decades after the suspension of Tesla's experiments).

Currently, WPT technology is of interest in scientific as well as industrial areas. Energy transfer efficiency is a central issue in WPT and ultimately imposes system coverage range, performance, and reliability. At the receiver side, the efficiency optimization of the radio-frequency (RF)–dc converter circuits is a must and is traditionally accomplished through improved circuit design [4]–[8].

Alternatively, the RF–dc conversion efficiency can be boosted by selecting a proper excitation signal [9]–[16]. For instance, the use of high-PAPR multisine signals has been proven to increase the efficiency of RF–dc circuits when compared with CW signals [8], [11].

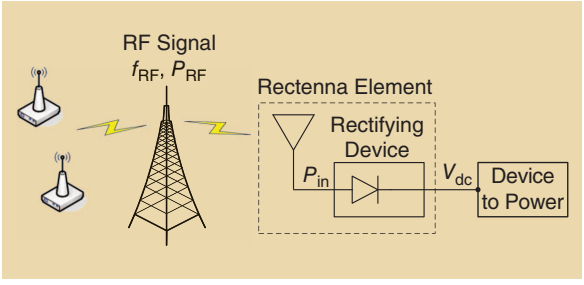

Figure 1. *A simplified schematic of a WPT system.*

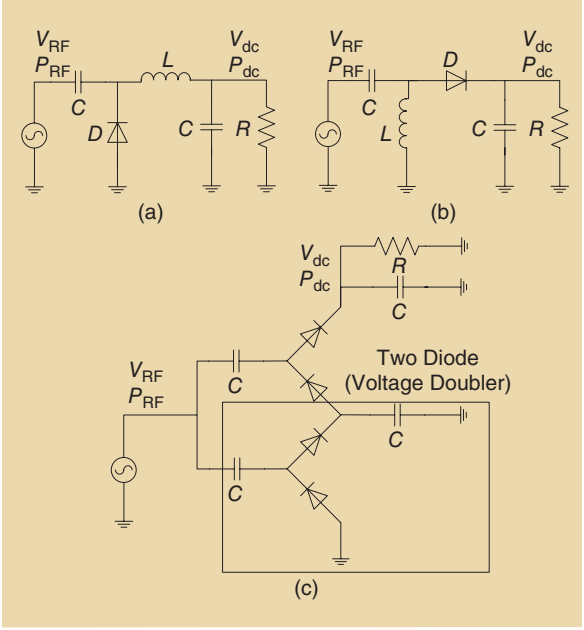

Figure 2. *The basic RF–dc converter topologies: (a) a single-shunt diode, (b) a single-series diode, and (c) a voltage multiplier (two level).*

Traditional Wireless Power Transfer Using CW Signals

Typically, the transfer of energy wirelessly is realized using a CW signal. The block diagram of a WPT system is shown in Figure 1. At the transmitter side, dc energy is converted into a CW RF signal, which is radiated through the transmitting antenna. The RF energy is collected by the receiving antenna and is forwarded to the RF–dc converter, which converts it back to dc energy to power up the electronic circuits.

CW RF–DC Conversion

The basic topologies of RF–dc converters or rectifier circuits are shown in Figure 2. The first two topologies (shunt and series diodes) are envelope detectors, which ideally provide an output dc voltage proportional to the input power (due to their predominant second-order behavior). The third configuration is a voltage multiplier or charge pump (in this case, a two-level one), which is used to boost the output voltage amplitude. Single-diode topologies are, in principle, more power efficient than charge pumps (Figure 3) and are often used in energy-harvesting circuits. On the other hand, charge pumps are capable of providing higher voltage levels and are commonly utilized in circuits that need voltage excursion rather than power efficiency, such as passive RF identification (RFID) tags.

The rectification of a CW signal using a single-diode rectifier is shown in Figure 4. Considering the exponential transfer-function characteristic of a rectifying diode ($I-V$ curve), a CW voltage signal at the input yields an output current signal with a certain dc component. On the other hand, if a high-PAPR signal (e.g., a multisine signal) is applied to the same device, this results in a higher-output dc component, even considering the same average power. This is shown in Figure 5.

Typical efficiency curves of different RF–dc converter circuits are shown in Figure 3. The RF–dc power efficiency is defined as the ratio between the output dc power (P_{out}) and the input RF power (P_{in}). From Figure 3, two conclusions can be drawn. First, the efficiency depends on the selected circuit topology, and the lower the number of devices, the higher the efficiency. This is because of the need for a minimum amount of input power to switch on the rectifying devices.

Second, the efficiency depends on the available power at the input of the circuit: for low power levels, the efficiency is low because the rectifying device is not completely switched on. As the input power

increases, the efficiency increases and reaches a maximum value right before the input amplitude reaches the diode breakdown voltage. After this point, the diode reverse current starts to be significant, and the efficiency drops. This power dependence imposes the necessity of optimizing the design for the expected input power level.

If the rectifying device is approximated by a fourth-order, even-order polynomial series [13], when a sinusoidal signal is used as input (1), the output dc component (after filtering) is given by (2)

$$x(t) = B\cos(\omega_1 t + \phi_1) \tag{1}$$

$$y_{dc} = \frac{B^2 k_2}{2} + \frac{3B^4 k_4}{8}. \tag{2}$$

This simple model considers only the first two even-order coefficients (k_2 and k_4) of the Taylor expansion. Assuming that the second order is dominant, the dc component can be approximated to be proportional to the square of the input signal amplitude, i.e., proportional to the average input power.

Unconventional Waveforms for WPT

To illustrate the rectification process of a high-PAPR signal and to show the mechanism by which the efficiency is improved over the single-carrier case, let us consider a high-PAPR multisine signal (Figure 5) as described in [13]. If such a signal is applied to the input of a rectifying circuit, the output dc component will be higher than a CW, even using the same average power. This is due to the higher voltage peaks exhibited by the multisine waveform, which are able to overcome the diode threshold barrier more efficiently than the (average) power-equivalent CW signal (Figure 5). Equation (3) is a four-tone, evenly spaced, multisine signal whose tones have amplitude A; phases φ_1, φ_2, φ_3, and φ_4; and frequencies ω_1, $\omega_2 = \omega_1 + \Delta\omega$, $\omega_3 = \omega_1 + 2\Delta\omega$, and $\omega_4 = \omega_1 + 3\Delta\omega$, respectively, where $\Delta\omega$ is the frequency spacing between the tones. After filtering out the RF and the baseband components, the dc output of a rectifier as modeled in [13] is given by (4)

$$\begin{aligned} x(t) &= A\cos(\omega_1 t + \varphi_1) + A\cos(\omega_2 t + \varphi_2) \\ &\quad + A\cos(\omega_3 t + \varphi_3) + A\cos(\omega_4 t + \varphi_4) \end{aligned} \tag{3}$$

$$\begin{aligned} y_{dc} &= \frac{4A^2 k_2}{2} + \frac{21A^4 k_4}{2} + \frac{3A^4 k_4}{2}\cos(2\varphi_3 - \varphi_2 - \varphi_4) \\ &\quad + \frac{3A^4 k_4}{2}\cos(-2\varphi_2 + \varphi_1 + \varphi_3) \\ &\quad + 3A^4 k_4 \cos(\varphi_1 - \varphi_2 - \varphi_3 + \varphi_4). \end{aligned} \tag{4}$$

By (4) it can be concluded that the output is a function of the input phases, and it can be optimized by choosing the adequate phase arrangement that maximizes the signal PAPR. The maximum PAPR value occurs when all of the tones are aligned with the 0° phase ($\varphi_1 = \varphi_2 = \varphi_3 = \varphi_4 = 0°$) or when the phase progression between adjacent tones is constant ($\phi_{i+1} - \phi_i = \Delta\phi$) [13]–[17]. Having equally spaced tone frequencies ($\omega_i = \omega_0 + i \cdot \Delta\omega$) is also a necessary condition.

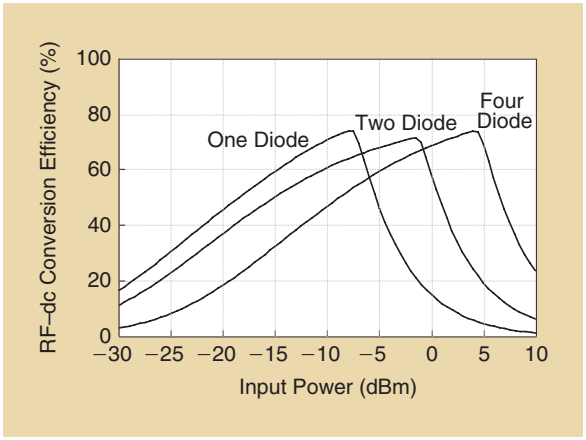

Figure 3. *The RF–dc conversion efficiency versus the RF input power level for different rectifier topologies.*

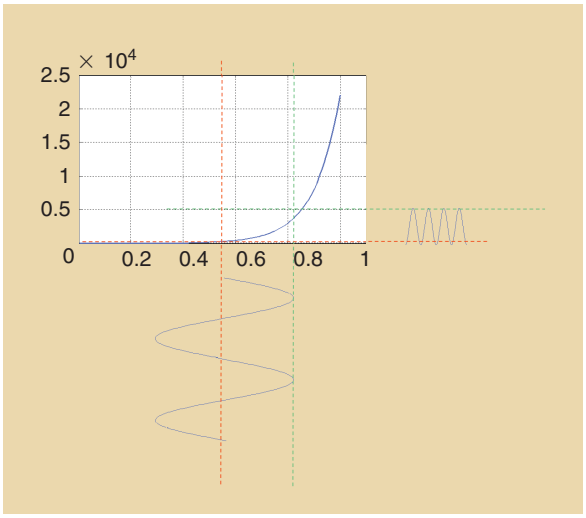

Figure 4. *The rectification of a sinusoidal signal.*

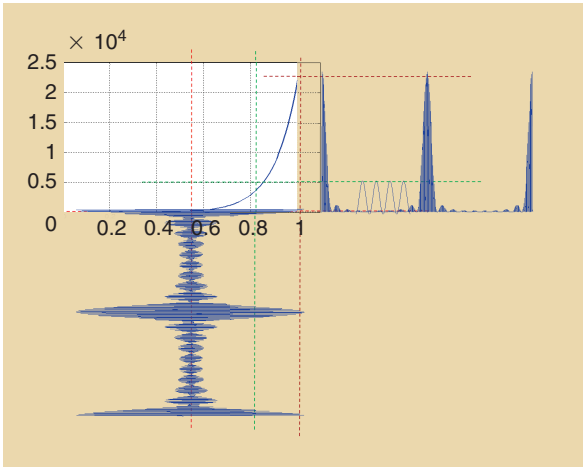

Figure 5. *The rectification of a high-PAPR multisine signal.*

Most research efforts to enhance the efficiency of wireless power transfer systems have been confined to the circuit-level design.

By increasing the PAPR of the multisine, the output dc voltage also increases due to the fact the PAPR peaks will charge the output capacitor to a higher value. However, a proper signal and circuit design is required to accommodate the increased voltage ripple imposed by the low-frequency component of the multisine envelope.

As multisine signals, a number of other signals that present high-PAPR characteristics can excite rectifying devices more efficiently than CW signals and will be studied in the next sections. These include, for instance, pulsed or ICW, chaotic, white-noise, multicarrier OFDM, UWB, and harmonic signals.

To evaluate the improvements obtained with the unconventional schemes, compared with the CW, a figure of merit is defined: the RF–dc efficiency gain (G_η), which relates the dc power collected from a single carrier with the dc power obtained with an unconventional waveform with the same average power ($P_{RF(CW)} = P_{RF(U)}$)

$$\begin{aligned} G_\eta(\text{dB}) &= 10 \cdot \log 10\left(\frac{\eta_{(U)}}{\eta_{(CW)}}\right) \\ &= 10 \cdot \log 10\left(\frac{\dfrac{P_{dc(U)}}{P_{RF(U)}}}{\dfrac{P_{dc(CW)}}{P_{RF(CW)}}}\right) \\ &= 10 \cdot \log 10\left(\frac{P_{dc(U)}}{P_{dc(CW)}}\right) \\ &= 10 \cdot \log 10\left(\frac{V^2_{dc(U)}}{V^2_{dc(CW)}}\right), \end{aligned} \tag{5}$$

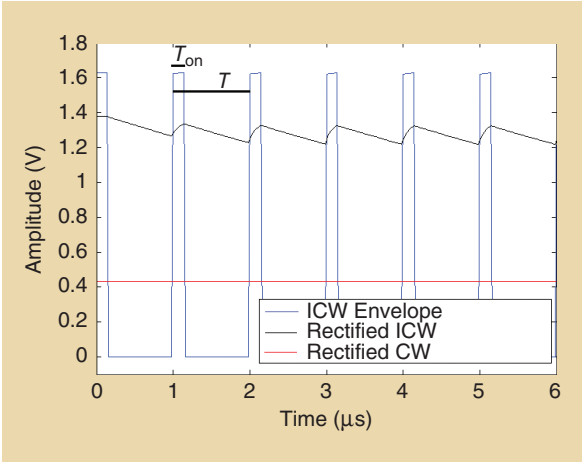

Figure 6. *The CW versus ICW signal, simulated time-domain waveform for the input ICW envelope (square wave), the rectified ICW output (signal with ripple), and the rectified CW output (constant signal).*

where $P_{dc(CW)}$ refers to the output dc power obtained in a rectifier circuit when using a single-carrier signal at its input and $P_{dc(U)}$ refers to the output dc power obtained when using an unconventional signal.

ICW

An early use of a nonconventional waveform to enhance WPT can be found in [9], where the CW signal of a UHF RFID reader was switched on and off with a given duty cycle: D is the ratio between the on time (T_{ON}) and the cycle period (T). This created a pulsed high-PAPR pattern, which enhanced the RF–dc conversion efficiency of the tag's rectifier circuits and, consequently, allowed the average radiated power to be reduced while keeping the same communication distance.

To evaluate this effect here, a series diode rectifier, similar to that in Figure 2(b), is fed either with a CW signal (with a constant amplitude equal to A) and with an ICW signal (with the on amplitude equal to B). Both signals are set to the same average power by calculating $B = A/\sqrt{D}$, and the output dc values are compared. As observed in Figure 6, the output voltage produced by a 15% duty cycle ICW signal (rippled signal) is much higher than that provided by a CW signal (constant signal) with the same average power. Tables 1 and 2 evaluate the dependency of the output dc voltage on the ICW duty cycle (D), input peak amplitude (B), and PAPR. As can be seen, the lower the duty cycle and the higher the input peak amplitude and PAPR, the higher the output voltage and efficiency gain. On the other hand, the increase in D causes an increase in the output ripple, and thus, a tradeoff should exist.

It is worth mentioning that, if a simultaneous power and data transfer is desired (e.g., in passive RFID), then the pulse envelope frequency must be higher than the intended data rate. In this example, a 1-GHz signal with 1-MHz square envelope is used.

UWB Signals

Following the same reasoning, UWB signals were proposed for an efficient low-power transmission [10], [11]. A train of short-duration pulses with relatively high amplitude exhibits a very low average power value (and consequently a high PAPR value). In [10], a conversion efficiency of 50% was achieved in a Schottky diode voltage doubler fed with a relatively low average power level of –3 dBm.

Chaotic Waveforms

In [14], the use of a chaotic generator was proposed as a way to create high-PAPR signals. A Colpitts-based circuit with only one active device (bipolar transistor BFP183W) is used to synthesize a chaotic waveform that has a high PAPR [Figure 7(a)]. As chaotic signals have a continuous and broadband frequency spectrum, it is necessary to filter them before their use in WPT systems to avoid radiating in restricted frequency bands.

The chaotic signal used in [14] is centered around 450 MHz and has a PAPR of approximately 6.8 dB [Figure 7(b)]. The performance of a rectifier circuit in terms of RF–dc conversion efficiency, when using this chaotic signal in comparison with a single-carrier signal at 450 MHz, is performed in [14]. The rectifier circuit is based on the SMS7630 Schottky diode and has an RF–dc conversion efficiency curve centered around 450 MHz [Figure 7(b)]. From Figure 7(c), it can be seen that the use of the chaotic signal leads to an improvement in the RF–dc conversion efficiency of the rectifier circuit of 20% compared with a single-carrier signal with the same average power of –6.5 dBm. As we reduce the input power level, the improvement in the RF–dc conversion efficiency is less dramatic but still one can obtain improvements in the order of 15% for –20-dBm input power.

Modulated Signals

In [15], different types of signals, including an OFDM and a white-noise-based signal, are considered for maximizing efficiency in WPT systems. In particular, the selected OFDM signal is a long-term evolution frequency division duplex downlink OFDM signal with 301 occupied subcarriers modulated using quaternary phase-shift keying (QPSK), 5-MHz bandwidth, and a PAPR of 12 dB. The white-noise-based signal is a band-limited signal around 433 MHz, and it is synthesized modulating a single carrier by a Gaussian white-noise signal provided by an arbitrary waveform generator Agilent 33250A source. The signal has a 1-Vpp amplitude and a PAPR of 13.7 dB. In both cases, the signals are filtered using a band-pass filter centered around 433 MHz and with a 3-dB bandwidth of 6 MHz.

TABLE 1. The CW input–output.

Input Amplitude, A (mV)	Input PAPR	Input Duty Cycle (D)	Output dc, V_{dc} (mV)	Gain ($G\eta$)
631	3 dB	1	434	0 dB

TABLE 2. The ICW input–output as a function of D and PAPR.

Duty Cycle (D) (%)	Input Amplitude $B = A/\sqrt{D}$ (mV)	Input PAPR = 10 log(2/D) (dB)	Output dc (mV)	Gain, $G\eta$ (dB)
100	631	3.0	434	
70	754	4.6	538	1.87
40	997	7.0	744	2.94
20	1,408	10.0	1,096	8.04
10	1,991	13.0	1,585	11.3

Energy transfer efficiency is a central issue in WPT and ultimately imposes system coverage range, performance, and reliability.

An experiment is performed in [15] where the performance of a rectifier circuit in terms of RF–dc conversion efficiency is evaluated for the previous two signals and also for a single-carrier signal. The carrier frequency for the three signals used in the experiment

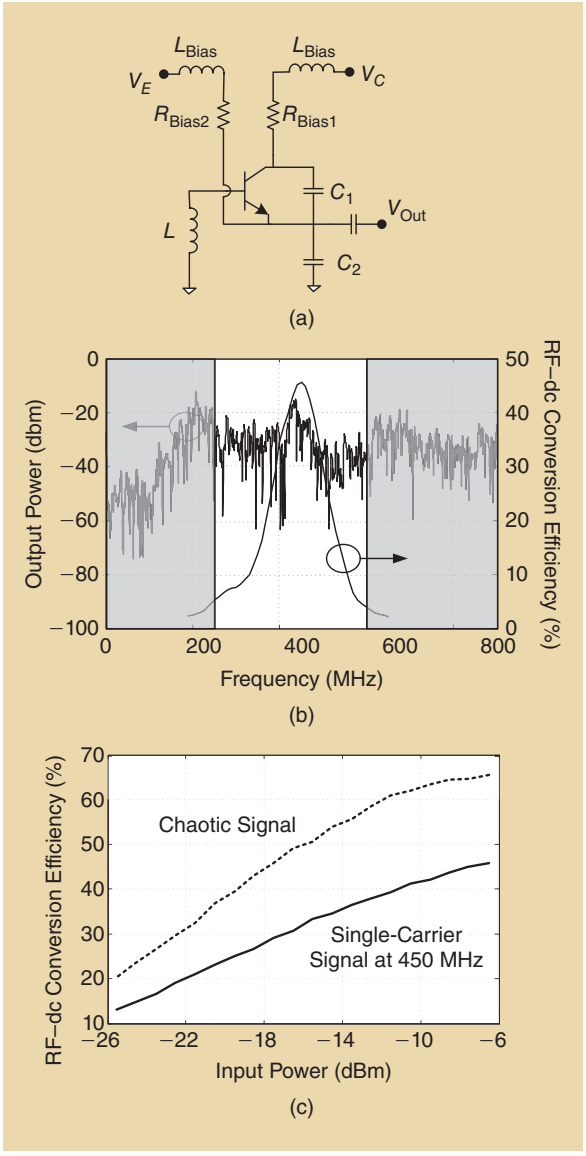

Figure 7. *The high-PAPR chaotic signals improve the RF–dc conversion efficiency in rectifier circuits: (a) the chaotic generator, (b) the frequency spectrum of the chaotic signal and RF–dc conversion efficiency of the rectifier circuit, and (c) a comparison of the RF–dc conversion efficiency when using chaotic signals and a single-carrier signal.*

The third configuration is a voltage multiplier or charge pump (in this case a two-level one), which is used to boost the output voltage amplitude.

is 433 MHz. The results demonstrate how high-PAPR modulated signals can obtain an improved performance in rectifier circuits compared with single-carrier signals and, consequently, are suitable for use in WPT systems [Figure 8(a)]. The complementary cumulative distribution function of the PAPR of the envelope of the signals shows that the OFDM signal, apart from having a higher maximum PAPR, also has a higher periodicity in the occurrence of the peaks in the signal [Figure 8(b)]. This fact leads to even a higher improvement in the RF–dc efficiency if compared with the white-noise-based signal.

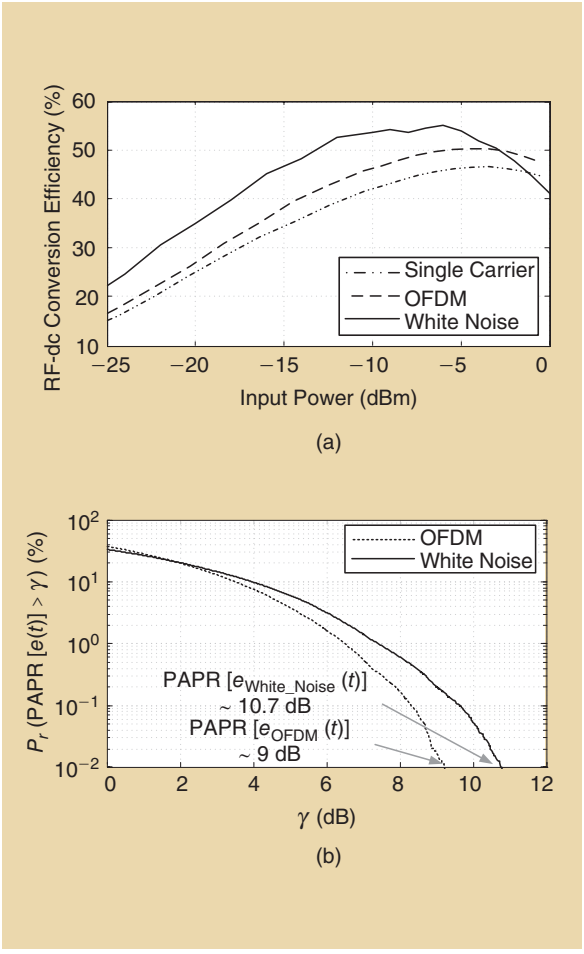

Figure 8. *An evaluation of the rectifier performance for different types of signals: (a) the RF–dc conversion efficiency of a rectifier centered around 433 MHz when using a single-carrier OFDM signal and a white-noise-based signal and (b) the complementary cumulative distribution function of the PAPR of the selected signals for the experiment.*

Multisines

Multisine signals, commonly used in OFDM communication systems, have been explored for their use in WPT. In [3]–[5], the reading range of UHF RFID tags was extended using a multisine scheme. In [7], the nonlinear behavior of RF–dc converters was investigated, and a mathematical model and description were presented to explain the efficiency enhancement in Schottky diode detectors when excited with high-PAPR signals. In the experiments conducted in [9] and [10], a multisine front end was integrated in a commercial RFID reader to extend its reading range.

Multisine Design

A multisine signal results from the combination of several sines with different amplitudes, frequencies, and phases. The choice of the individual tone characteristics determines the shape of the multisine time-domain waveform. As stated before, to achieve the maximum PAPR, a proper phase arrangement must be selected. Beyond phase

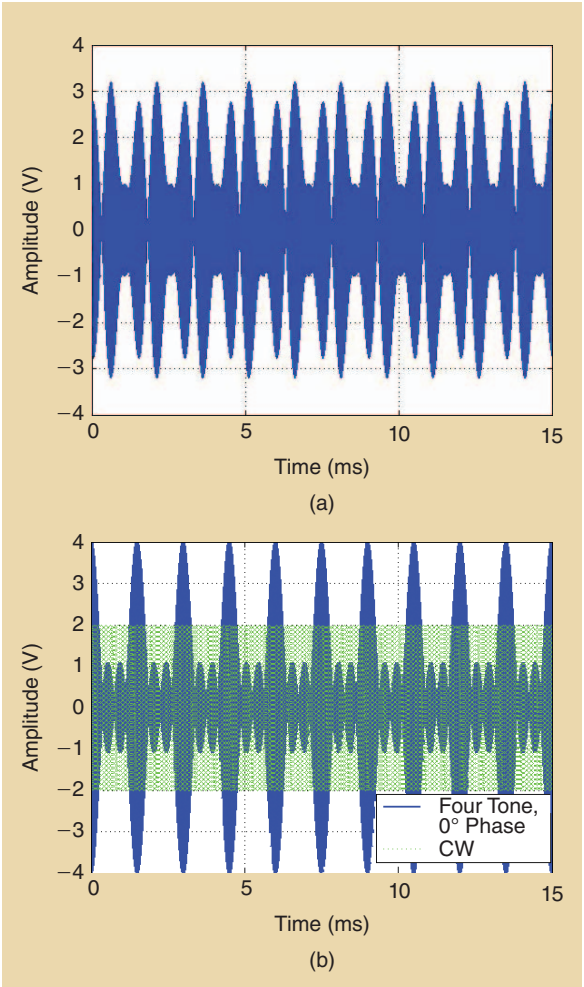

Figure 9. *Time-domain waveforms: (a) the four-tone multisine with a random phase arrangement and (b) the four-tone with 0° phase arrangement overlapped with a CW with the same average power.*

optimization, further optimization can be done by playing with the individual tone amplitudes and frequency separation. For instance, in [16], Gaussian formats were obtained using a specially designed algorithm.

A four-tone multisine signal, centered (center frequency and tone spacing only for illustration purposes) at 100 kHz with a tone spacing of 667 Hz and with a random phase arrangement, is shown in Figure 9(a). In Figure 9(b), the time-domain waveform of a four-tone signal with a 0° phase is shown, overlapped with a CW with the same average power [$A_{CW} = \sqrt{N} * A_{Tone}$, where A_{Tone} is the amplitude of the individual tones of (3) and N is the number of tones, $N = 4$]. While the random phase signal exhibits low peak values and low PAPR, the 0° phase signal presents a much higher PAPR than the CW signal and, consequently, will provide a higher rectified dc output.

Measured Efficiency Gain Results

Measurements were conducted to evaluate the efficiency gains obtained with several multisine signals.

The efficiency depends on the available power at the input of the circuit.

Two RF–dc converter circuits where tested: a single-diode detector [Figure 9(a)] [13], commonly used for energy harvesting and WPT, and a five-stage charge pump or voltage multiplier typically used in passive RFID tags [Figure 9(b)] [17]. The two circuits operate in the 2.3-GHz and 866-MHz band, respectively. The RF–dc converters are first fed with a CW signal and, afterward, with a multisine signal with the same average power as the CW signal. The converter circuits are tested over a range of input power, input signal bandwidth, and phase arrangement of the multisine.

Figures 10–12 provide the dc voltage measurements and the efficiency gain as defined by (5). The measurement results support the initial premise that multisine signals provide an efficiency gain over CW signals.

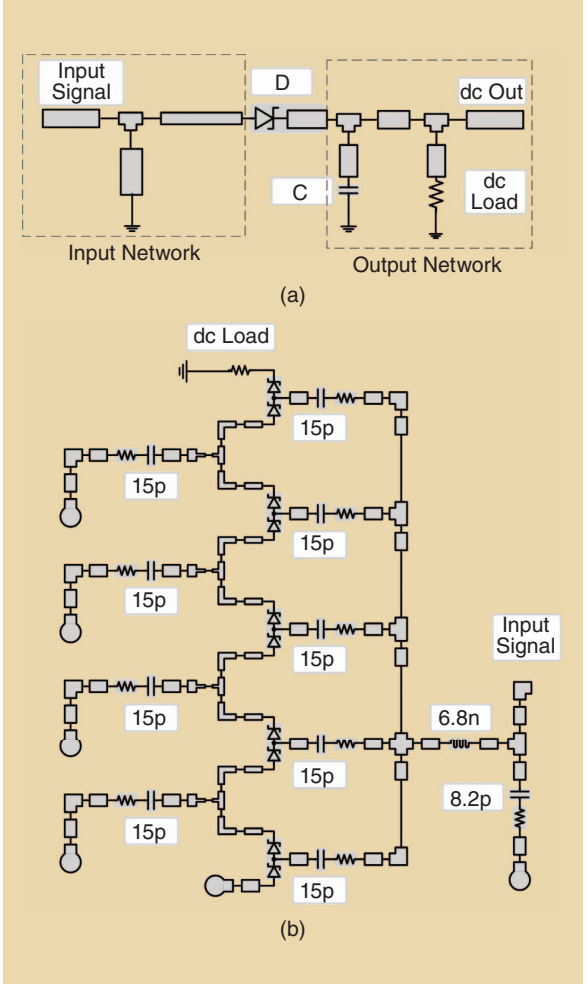

Figure 10. *The rectifying circuits constructed for tests: (a) a single-diode rectifier operating at the 2.3-GHz band and (b) a charge pump circuit operating at 866 MHz.*

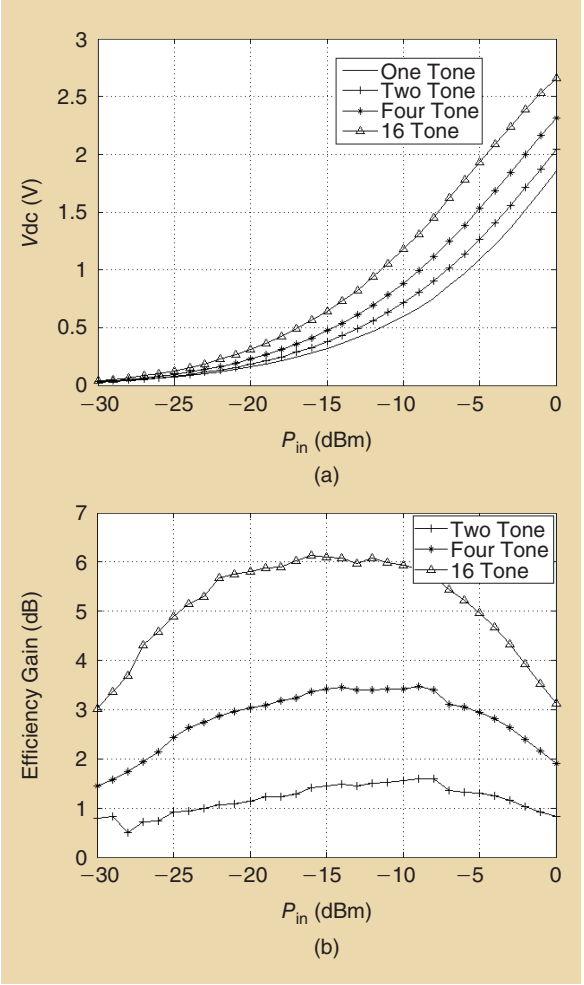

Figure 11. *The single-diode rectifier measurements: (a) the dc voltage as a function of the input power and (b) the efficiency gain as a function of the input power.*

The output dc component will be higher than a CW, even using the same average power.

This is true for both the single-diode rectifier as well as for the charge pump circuit, and in the second case, it explains the range improvements in passive RFID systems reported in [12] and [19].

Harmonically Spaced Multisines

Multisine signals are usually designed to operate on a single band to keep the matching procedure simple at the receiver side. However, to provide a high-PAPR signal, many subcarriers are needed, and thus, the frequency spacing between each subcarrier gets significantly lower as the number of subcarriers increases. This kind of signal is characterized by having an envelope that has a peak power period equal to the inverse of the subcarriers spacing frequency.

The output low-pass filter needs a high time constant to filter out the low-intermodulation products that are generated in the rectification process and to avoid a large output ripple that would reduce the dc level generated. Usually, low-pass filters are simple resistor-capacitor circuits. Increasing the capacitor value might not be a good idea since high-value capacitors are known to have bad behavior at high frequencies, and increasing the value of the load enables us to obtain more dc voltage but reduces the available dc output power. To prevent such phenomena, a multiband RF–dc converter is considered and tested in this section to obtain a higher frequency spacing between each subcarrier, as shown in Figure 13. If the bands are harmonically spaced, the resulting time-domain signal has the same peak voltage of a single-band multisine. Moreover, it has the same peak voltage frequency of a CW at the same frequency. Figure 14 shows such a signal.

The most challenging issue of using these signals is the matching procedure at the receiver. For two

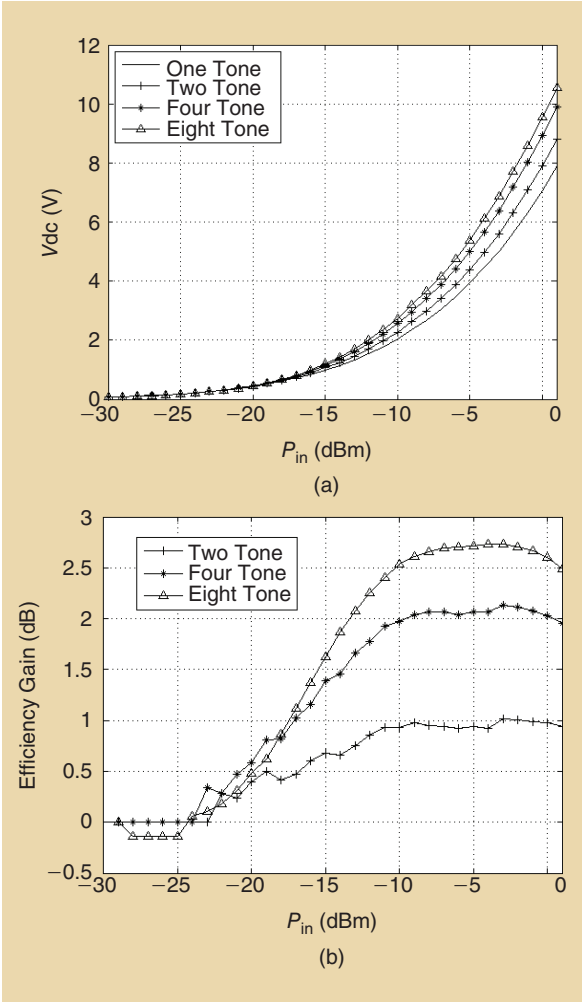

Figure 12. *The charge pump rectifier measurements: (a) the dc voltage as a function of input power and (b) the efficiency gain as a function of the input power.*

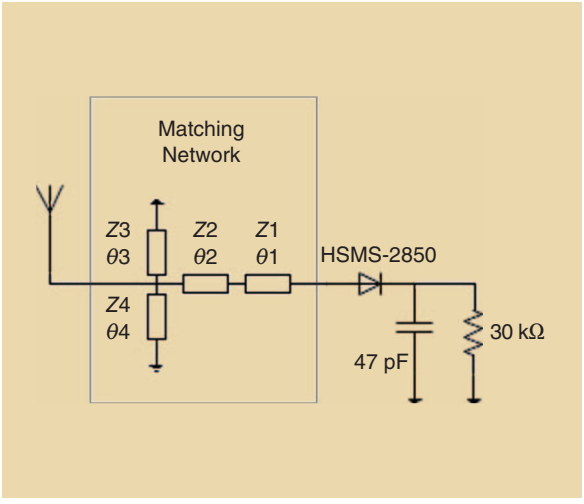

Figure 13. *The proposed dual-band RF–dc converter.*

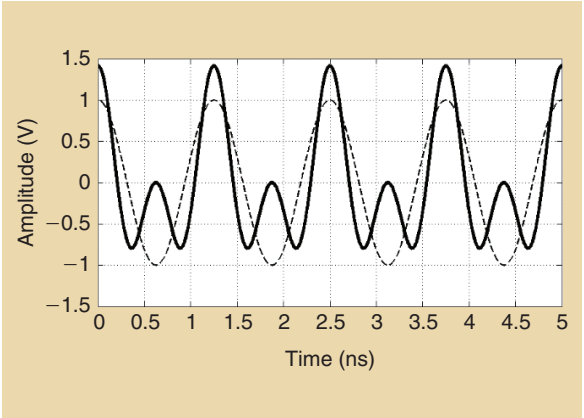

Figure 14. *The time-domain waveforms of a CW at 900 MHz and a harmonically spaced multisine with two subcarriers at 900 and 1,800 MHz with the same total power.*

subcarriers, similar to the single-stub matching network at a single frequency, two sections of transmission lines are connected in series with the circuit and transform its input impedances to normalized unit conductance at the two designated frequencies simultaneously. The resulting susceptances are then canceled out by a two-shunt stub at the two frequencies, as shown in Figure 13 [22]. The circuit was then optimized for the two bands and for –15 dBm of the total input power (Figure 15).

The simulated results when excited with different signals are shown in Figure 16. It is possible to check that the harmonically spaced multisine provides the best results in terms of dc output voltage and power conversion efficiency considering all excitation signals with the same power. This is due to the better synergy between the output filter time constant and the input peak voltage period. The 30-kΩ load was chosen to maximize both the voltage gain and power conversion efficiency.

It is possible to observe that this kind of signal enables the rectifier to generate more dc voltage at higher input powers, virtualizing a larger diode breakdown voltage. The resulting time-domain waveform of the harmonically spaced multisine is asymmetric, providing a high positive peak voltage and lower negative peaks as the number of harmonics increases. If we look at the receiver, subcarriers must arrive at the diode's input at a 0° phase arrangement to show a high PAPR. As it is, the phase synchronism at the transmitter must be calibrated based on the amount of phase shift that each subcarrier suffers on the matching network as subcarriers are quite separated in frequency. On this simulation, a phase shift of 200° was needed between carriers at the source to provide the maximum PAPR at the diode's input. More progress is being made on this approach, and more results are expected in the near future.

Discussion: Pros and Cons of Each Approach

The approaches presented in this article present a tradeoff between the efficiency and the spectrum occupancy, system complexity, and generation approaches.

ICW

The disadvantage of the ICW solution is the spectral inefficiency caused by spectrum regrowth (due to the intermittent regime). At least some low-pass filtering should be applied to the intermittent pattern before transmitting the signal, which can reduce the predicted PAPR.

UWB

The main drawback of the UWB approach is the increased spectral bandwidth and the need for wideband antennas and components. Furthermore, contrary to multisine signals that can be incorporated into

The output voltage produced by a 15% duty cycle ICW signal (rippled signal) is much higher than that provided by a CW signal.

conventional RFID systems (as was done in [12] and [18]–[19]), the UWB scheme cannot be directly applied to these systems, which are narrowband. Ultrawideband circuits are needed.

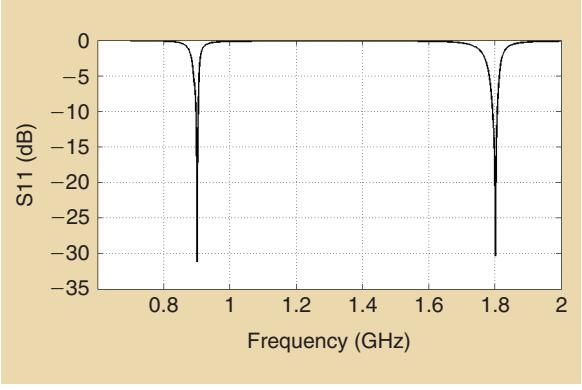

Figure 15. *The simulated S11 of the dual-band RF–dc converter with −15 dBm of input power.*

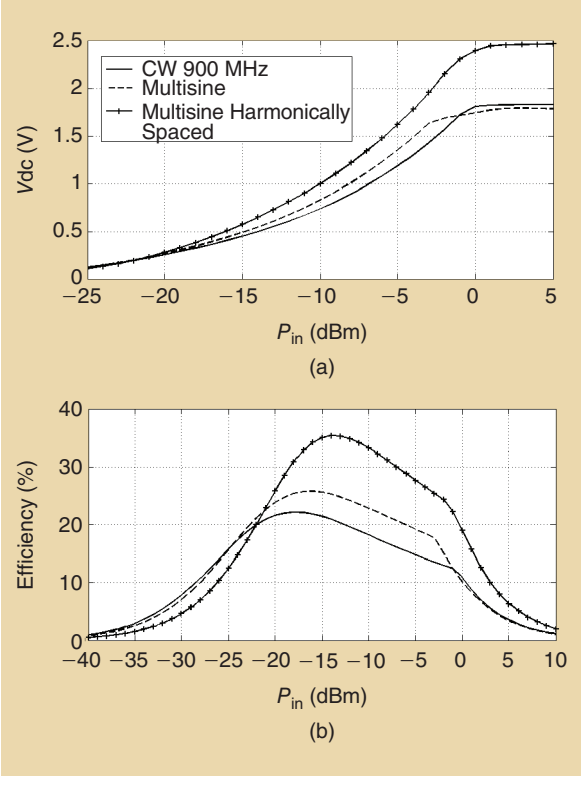

Figure 16. *The simulated results when excited with a 900-MHz CW, an 899 + 901-MHz multisine, and a 900 + 1,800-MHz multisine: (a) the output dc voltage generated and (b) the power conversion efficiency achieved.*

The use of a chaotic generator was proposed as a way to create high-PAPR signals.

Chaotic Signals

As a disadvantage, chaotic signals have a continuous and broadband spectrum, so it is necessary to filter them to avoid radiating in restricted or not allowed frequency bands. On the other hand, synthesizing chaotic waveforms can be less complex than synthesizing other types of signals; an example is the chaotic generator of [14] where a single active device circuit suffices.

Multisines

It is necessary to generate multicarrier components, which increase the complexity of the transmitter (unless envelope amplification techniques such as envelope tracking are used). The rectifier must accommodate the multisine signal bandwidth. A generation alternative was presented in [20] and [21] that can overcome some of these challenges by space power combining sines in the air interface.

In all cases, the amplification of high-PAPR signals is challenging and requires efficient approaches to amplify and transmit such high-PAPR signals. For instance, in [21], two architectures were proposed to efficiently create high-PAPR multisines. The first consists of individually transmitting single-tone signals that are externally locked to a common reference signal to establish a phase reference. The second is based on mode-locked oscillator schemes, where no external reference is required but advantage is taken of the synchronization phenomena to establish the phase reference.

Harmonic Signals

There is a need for multiband circuit design at the receiver side, and the generation of harmonic multifrequency signals at the transmitter is required. The rectifier device is required to operate in the selected frequency harmonics. Nevertheless, the preliminary results show that these are probably the signals that achieve better results in conventional RF–dc converters.

References

[1] A. A. Huurdeman, *The Worldwide History of Telecommunications*. Hoboken, NJ: Wiley, 2003.

[2] N. Tesla, *The Transmission of Electric Energy Without Wires* (The Thirteenth Anniversary Number of the Electrical World and Engineer). New York: McGraw-Hill, Mar. 5, 1904.

[3] E. F. W. Alexanderson. (2015, Feb. 3). IEEE Global History Network. [Online]. Available: http://www.ieeeghn.org/wiki/index.php/Ernst_F._W._Alexanderson

[4] W. C. Brown, "Electronic and mechanical improvement of the receiving terminal of a free-space microwave power transmission system," Raytheon Company, Wayland, MA, Tech. Rep. PT-4964, NASA Rep. CR-135194, Aug. 1977.

[5] A. Georgiadis, G. Andia, and A. Collado, "Rectenna design and optimization using reciprocity theory and harmonic balance analysis for electromagnetic (EM) energy harvesting," *IEEE Antennas Wireless Propagat. Lett.*, vol. 9, pp. 444–446, July 2010.

[6] Z. Harouni, L. Osman, and A. Gharsallah, "Efficient 2.45 GHz rectenna design with high harmonic rejection for wireless power transmission," *IJCSI Int. J. Comput. Sci. Issues*, vol. 7, no. 5, p. 424, Sept. 2010.

[7] K. Hatano, N. Shinohara, T. Mitani, K. Nishikawa, T. Seki, and K. Hiraga, "Development of class-F load rectennas," in *Proc. Int. Microwave Workshop Series Innovative Wireless Power Transmission: Technologies, Systems, Applications*, 2011, pp. 251–254.

[8] R. Scheeler, S. Korhummel, and Z. Popovic, "Daul-frequency ultralow-power efficient 0.5g rectenna," *IEEE Microwave Mag.*, vol. 15, no. 1, pp. 109–114, 2014.

[9] H. Matsumoto and K. Takei, "An experimental study of passive UHF RFID system with longer communication range," in *Proc. Asia-Pacific Microwave Conf.*, 2007, pp. 1–4.

[10] L. Chun-Chih, Y. Yu-Lin, T. Chi-Lin, L. Chieh-Sen, and Y. Chin-Lung, "Novel wireless impulsive power transmission to enhance the conversion efficiency for low input power," in *Proc. Microwave Workshop Series Innovative Wireless Power Transmission*, 2011, pp. 55–58.

[11] Y. Yu-Lin, Y. Chin-Lung, T. Chi-Lin, and L. Chieh-Sen, "Efficiency improvement of the impulsive wireless power transmission," in *Proc. Microwave Workshop Series Innovative Wireless Power Tansmission*, 2011, pp. 175–178.

[12] M. S. Trotter, J. D. Griffin, and G. D. Durgin, "Power-optimized waveforms for improving the range and reliability of RFID systems," in *Proc. IEEE Int. Conf. RFID*, 2009, pp. 80–87.

[13] A. S. Boaventura and N. B. Carvalho, "Maximizing dc power in energy harvesting circuits using multisine excitation," in *Proc. Int. Microwave Symp.*, Baltimore, MD, June 2011, pp. 1–4.

[14] A. Collado and A. Georgiadis, "Improving wireless power transmission efficiency using chaotic waveforms," in *IEEE MTT-S Int. Microwave Symp. Dig.*, Montreal, QC, Canada, June 2012, pp. 17–22.

[15] A. Collado and A. Georgiadis, "Optimal waveforms for efficient wireless power transmission," *IEEE Microwave Wireless Compon. Lett.*, vol. 24, no. 5, pp. 354–356, May 2014.

[16] N. B. Carvalho, K. A. Remley, D. Schreurs, and K. C. Card, "Multisine signals for wireless system test and design," *IEEE Microwave Mag.*, vol. 9, no. 3, pp. 122–138, June 2008.

[17] R. D. Fernandes, N. B. Carvalho, and J. N. Matos, "Design of a battery-free wireless sensor node," in *Proc. IEEE EUROCON—Int. Conf. Computer Tool*, Apr. 27–29, 2011, pp. 1–4.

[18] C. R. Valenta and G. D. Durgin, "Rectenna performance under power-optimized waveform excitation," in *Proc. IEEE Int. Conf. RFID*, Apr. 30–May 2, 2013, pp. 237–244.

[19] A. S. Boaventura and N. B. Carvalho, "Extending reading range of commercial RFID readers," *IEEE Trans. Microwave Theory Tech.*, vol. 61, no. 1, pp. 633–640, Jan. 2013.

[20] R. A. York and R. Compton, "Coupled-oscillator arrays for millimeter-wave power-combining and mode-locking," in *Proc. IEEE Int. Microwave Symp.*, Albuquerque, NM, 1992, pp. 429–432.

[21] A. S. Boaventura, A. Collado, A. Georgiadis, and N. B. Carvalho, "Spatial power combining of multi-sine signals for wireless power transmission applications," *IEEE Trans. Microwave Theory Tech.*, vol. 62, no. 4, pp. 1022–1030, 2014.